ELSEVIER

Earth and Planetary Science Letters 168 (1999) 145–158

EPSL

Long-τ VRM and relative paleointensity estimates in sediments

Yvo S. Kok [a,*], Lisa Tauxe [b]

[a] *Fort Hoofddijk Paleomagnetic Laboratory, Budapestlaan 17, 3584 CD Utrecht, Netherlands*
[b] *Scripps Institution of Oceanography, La Jolla, CA 92093-0220, USA*

Received 14 November 1998; revised version received 16 February 1999; accepted 16 February 1999

Abstract

Geomagnetic paleointensity measurements from sedimentary records can be severely affected by viscous remanent magnetization (VRM). We present a method for determining varying amounts of long-term VRM acquired during the present polarity interval, using the typically non-linear relationship between acquisition of artificial magnetization and demagnetization of NRM. The non-linear parts are to be avoided for paleointensity determinations, but here we focus on their use for indicators of long-relaxation time VRM. The method, which does not require determining paleointensity values, suggests correlations with paleoclimate curves and age-dependent growth of VRM. Furthermore, it appears that the long-τ VRM acquired during the Pleistocene is accompanied by short-τ effects detected in the laboratory environment.

Keywords: paleomagnetism; magnetic intensity; natural remanent magnetization; viscous remanent magnetization; Brunhes Epoch

1. Introduction

In paleomagnetism, the natural remanent magnetization (NRM) of rocks consists of a primary magnetization acquired during formation of the rock, which is often overprinted by secondary magnetizations. The NRM of volcanic rocks is formed by cooling below the Curie temperature of the magnetic material (thermo-remanent magnetization or TRM), whereas sedimentary rocks have a more complicated process of natural magnetization referred to as detrital remanent magnetization (DRM) and/or post-depositional processes (pDRM). Here we consider the entire continuum of physical processes during deposition, compaction and burial as DRM (see [1]).

Viscous remanent magnetization (VRM) is one of the unwanted remanences, which must be eliminated from NRM in order to characterize the properties of the primary remanence. The removal of VRM and other secondary magnetizations is the main purpose of demagnetization methods in use for both directional and intensity studies. Information about the intensity of the primary remanence, and thus an indication of the paleomagnetic field strength, is the most difficult to obtain. For thorough discussions of viscous magnetization we refer to, e.g., [2–6]. The important aspects of VRM are briefly summarized here.

According to Néel [2] any initial remanence M_0 will asymptotically approach its equilibrium magne-

* Corresponding author. New address: CEREGE, Université Aix-Marseille III, B.P. 80, 13545 Aix-en-Provence Cedex 04, France. Fax: +31 30 253 1677; E-mail: yvoskok@geo.uu.nl

0012-821X/99/$ – see front matter
PII: S0012-821X(99)00041-2

tization M_e in an exponential fashion with a characteristic constant known as the relaxation time τ, which strongly depends on grain size, coercivity and temperature. Any naturally occurring assemblage of magnetic particles will have a range of relaxation times. When viewed over a restricted time span, the behavior of VRM can often be reasonably approximated by some $\log(t)$ relation, where t is time (see e.g., [2,7]). This approximation cannot hold when $t \to \infty$, for that would imply an infinite magnetization. Clearly, the longer a sample stays in a steady non-zero field, the more long-τ VRM is acquired and the closer to M_e its magnetization becomes.

The VRM intensity in paleomagnetic data is also driven by the type of magnetic material present in the rock. Differences in sediment composition inevitably cause changes in the magnetic properties and thus in the type and amount of VRM.

Since relaxation of magnetic remanence is a thermal activation process, elevated temperatures promote viscous behavior, i.e., acquisition or decay of VRM. The principle of thermal demagnetization of rocks rests on the consequence of the logarithmic reduction of the relaxation time on increased temperature. For example, a viscous remanence carried by particles with relaxation times of less than a few million years at room temperature can be erased at 200ºC within a few minutes (see [8]). Néel's blocking approximation of this process states that when $t < \tau$ no viscous relaxation has occurred, whereas at $t > \tau$ the equilibrium magnetization has been reached. While this is a good approximation on laboratory time scales (grains are either blocked or not), it is a rather poor approximation for geological time scales. It is important to remember that the populations of particles with relaxation times longer than the 'exposure' time t have also undergone some degree of relaxation. Furthermore, when the relaxation time is equal to the exposure time, only 63% of the maximum possible magnetization has been reached.

For rocks that have experienced only the present polarity chron, a viscous remanence will be added to the direction of the primary remanence vector. Of course, if the settings of lavas or sediments change, for instance because of tectonics, the secondary component can be in a different direction from the primary vector. Sediments or lavas older than 778 kyr have experienced the two antipodal states of the geomagnetic field, and have therefore also acquired VRM in the direction opposite to the primary direction. If such magnetizations are not effectively demagnetized, NRM values spanning a paleomagnetic reversal are expected to be offset. Earlier, we argued [9] that VRM carried in part by particles with relatively long relaxation times ($\tau > t$) may have caused the asymmetrical saw-toothed pattern observed around polarity reversals in sedimentary paleointensity records [10]. More effective demagnetization methods indicated that the saw-toothed pattern in one of the original records disappeared [11].

We emphasize that here we are mainly concerned with viscous remanent magnetization acquired by populations with long relaxation times over geological time ($\tau > t$). We refer to this type of VRM as long-τ VRM. Short-τ VRM acquired during collection, transportation or in the laboratory is often easily eliminated, but long-τ VRM is more persistent and may therefore not always be recognized. Moreover, long-relaxation time viscosity applies to *every* grain-size population of magnetic particles, because of thermal activation and is consequently more difficult to remove.

In this study, we put forward a method which yields an estimate for what we interpret as the amount of long-τ VRM from the present polarity chron. It uses sedimentary data from two Brunhes-age cores chron that have been used for paleointensity research. The long-τ VRM is compared with short-τ viscosity effects in the laboratory.

2. Paleointensity and VRM

There are two main types of stepwise demagnetization used in paleomagnetic studies: exposure to increasing temperatures or to increasing alternating fields. One standard technique in paleomagnetism involves the measurement of the NRM after a given demagnetization level ('blanket' demagnetization), at which it is assumed that VRM and other secondary magnetizations have been erased. In this way, it is hoped that a primary magnetization has been isolated. In paleointensity studies of sediments, this remanence is subsequently normalized by a bulk magnetic property to account for changes in magnetizability. The blanket normalization procedure assumes magnetic uniformity throughout the record. Changes in the bulk properties through diagenesis or environmentally controlled changes can violate the assumption of uniformity, resulting in compromised relative paleointensity estimates. Only when the bulk magnetic parameters (the normalizing factors) account for the primary non-geomagnetic factors that influence the NRM intensity, the ratios (NRM/normalizer) give reliable estimates of variations in the geomagnetic field intensity (see Tauxe [1] for a review on paleointensities).

2.1. Pseudo-Thellier and VRM

Conventional relative paleointensity estimates rely on NRM derived from bulk demagnetization at a single step. Often, several normalizers are used to assess magnetic uniformity (see e.g., [12]), but mostly this is done for a single NRM measurement. However, the blanket demagnetization step can be insufficient to remove variable amounts of VRM. The problem with using the traditional methods for relative paleointensity estimates is that it is impossible to assess the contribution of VRM to NRM in which the DRM and VRM are sub-parallel.

For volcanic rocks, a more sophisticated normalization method existed long before sedimentary sequences were used for paleointensity determination [13,14]. The Thellier–Thellier method uses thermal demagnetization of NRM and compares it with partial thermal remanences acquired in a known laboratory field at the same temperature steps. By plotting NRM remaining against the laboratory TRM, it is possible to separate components dominated by VRM from those that can be considered to be primary components. During the process, one is also able to monitor possible changes in magnetic parameters caused during the laboratory treatment. Absolute paleointensities can only be obtained from this method when the specimen has a thermoremanent (TRM) origin. Deep-sea sediments can also be subjected to the Thellier–Thellier method with promising results (see e.g., [15]. Although the DRM acquisition process is completely different from thermoremanent magnetization, the Thellier-paleointensities from sediments can at least be considered to be relative measures of the paleomagnetic field.

Recently, a pseudo-Thellier approach was developed for estimating relative paleointensities in sediments [16]. It uses non-destructive alternating fields (AF) demagnetization and anhysteretic remanent magnetization (ARM) acquisition as opposed to thermal methods in the Thellier–Thellier experiment. They suggested that the pseudo-Thellier technique is capable of separating VRM from DRM. Differences between the two paleointensity estimates were therefore taken to be measures of long-τ viscous effects during the Brunhes. These correlated with viscous behavior on a laboratory time scale [16].

2.2. VRM area model

We explore here the pseudo-Thellier method for detecting and quantifying long-τ VRM contributions parallel to the DRM. A schematic representation of an Arai plot [17] is given in Fig. 1. NRM (vertical axis) is plotted versus an artificially acquired anhysteretic remanence (ARM) at the same AF peak field (horizontal axis). A linear relation between the two assumes that ARM reasonably mimics DRM. The slope is used as an estimate of relative paleointensity, as is done in the Thellier–Thellier procedure for absolute determinations. If the VRM adds to the DRM, this will result in a higher value for NRM, while the magnetic parameter ARM remains unchanged. The VRM component causes the curve connecting the data to become concave up. After the demagnetization level at which the VRM is eliminated (as well as part of the DRM), only the primary NRM — i.e. DRM — will be further demagnetized. Ideally, the relation between ARM and DRM is linear; however, as Tauxe et al. [16] noted, it may be possible that they will never relate in this way. Please note that only VRM acquired in the same direction as DRM will behave in this way; when VRM is opposite to DRM the curve in the Arai plot can be concave down. For this study only Brunhes age sediments are used, however.

The vertical axis indicates the sum of DRM and VRM. One way to quantify the relative proportion of VRM to the NRM would be to calculate the slope of the best-fit line through the data and determine the y-intercept on the NRM axis (see Fig. 1). However, this procedure implicitly requires that the ‘real’ relative paleointensity has been reliably deter-

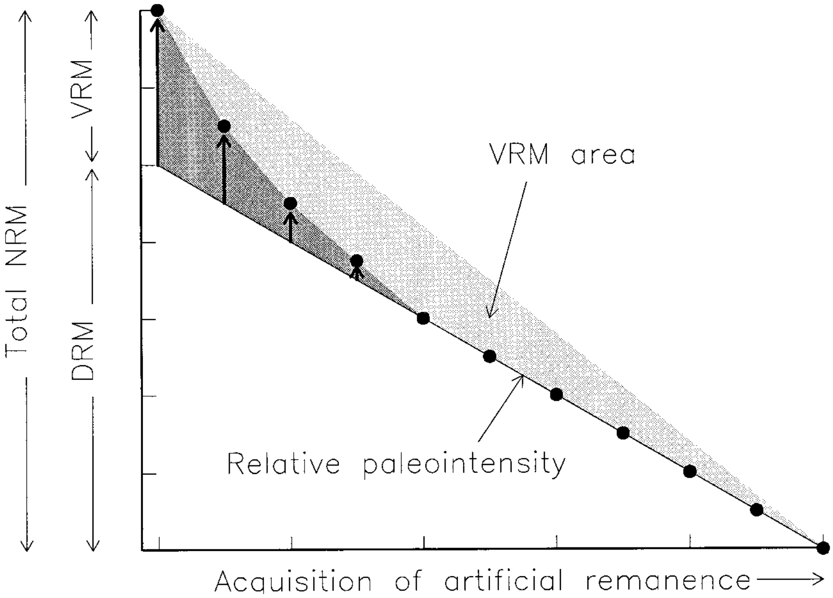

Fig. 1. Representation of Arai plot with best-fit slope as a relative measure of paleointensity and the 'VRM area' (light gray) as a first-order indication of the amount of VRM. The total NRM comprises DRM and VRM; a separation of the two remanences could ideally be found as the y-intercept of the relative paleointensity slope (see text).

mined, preferably with a very small error. Thus, the VRM estimate depends on the paleointensity estimate. The dark gray area in Fig. 1 is also a possible candidate for a VRM estimate. But similar to the y-intercept problems, we first have to know our true 'best-fit line'. Therefore, to calculate the dark gray area strongly depends on what is 'forced' to be the paleointensity slope.

To avoid this imposition, we choose to calculate the amount of VRM in a different manner. We determine the so-called 'VRM area' (indicated as the light gray area in Fig. 1), which has the advantage that it does not require that the paleointensity slope is known. The VRM area is the complement of the area under the curve, which is calculated as a Riemann sum (i.e., the sum of the areas of the columns with as widths the difference of two successive acquisition steps, and heights the average of two successive NRM demagnetization steps). Because not all specimens have identical volumes, we choose to normalize the VRM area by the area of the right triangle that spans the entire Arai plot (i.e. 0.5 × base × height = $0.5 \times NRM_{max} \times ARM_{max}$). Thus, the VRM area reflects the proportion of VRM in the NRM and not an absolute value. The VRM area will increase when the VRM contribution becomes more prominent, but this process is non-linear. Therefore, we concede that the VRM area cannot serve as an exact measure of the amount of VRM, nor is it applicable for very inhomogeneous cores. For example, if a record displays an occasional large, but soft, viscous overprint it will disappear early in the demagnetization process, but causes the VRM area to be rather large. Other samples that lack such soft VRMs will give a drastically different answer. Such soft VRM are not very important magnetizations for relative paleointensity studies, because they are routinely removed by storage in magnetically shielded space or low-field demagnetization treatment. What concerns us here is the more resistant long-τ VRM. It should be noted that part of the variations in the VRM area could reflect contributions from diagenetic effects, possibly as a time-dependent chemical remanence.

2.3. Material and methods

2.3.1. Core selection

We have resampled two cores (listed in Table 1), which in earlier studies passed the requirements for paleointensity determinations (e.g. [12]). The first

Table 1
Characteristics of the records used in this study

Core	Depth (m)	Length (m)	Latitude	Longitude	Age interval (ka)
ERDC 89p	1963	6.92	0º00.2′S	155º51.9′E	123–436
RNDB 75p	3078	8.10	1º54′N	160º12′E	142–672

core was taken during the Eurydice (ERDC) Expedition in 1975 from the Ontong–Java Plateau [18]. The remanence is carried by stable pseudo-single domain magnetite and the core is relatively uniform with respect to grain size and concentration. Its normalized record is therefore taken to reflect variations in the intensity of the geomagnetic field. From the same region, a second core was recovered during the Roundabout (RNDB) Expedition in 1988 [19]. Again, uniformity in the magnetic properties is observed, although a shift to less ideal conditions distinguishes the upper half from the lower half, but the criteria for obtaining paleomagnetic information are still met for the latter. The two cores have been dated by correlating their oxygen isotope records to a standard δ^{18}O curve [20] (with the Matuyama–Brunhes boundary adjusted to 780 ka [21]). In this study, the sediments have only witnessed the Brunhes polarity period, and therefore acquired long-τ VRM in a similar direction as the primary component. Furthermore, all samples were stored in a shielded room prior to measurements.

2.3.2. Paleointensity and error estimates

The pseudo-Thellier experiments took place at Fort Hoofddijk, where the remanence measurements were done on CTF and 2G cryogenic magnetometers. Alternating field demagnetization and ARM acquisition were performed on an SI-4 single axis instrument (with an optional 50 μT DC field) and the laboratory-built AF equipment (with an optional 42 μT background field). Error estimates for the best-fit slope in the Arai-plots were obtained by a jackknife resampling scheme. Relative paleointensity results with 90% confidence bounds for the two cores studied are shown in Fig. 2.

2.3.3. IRM experiments

Two types of isothermal remanent magnetization (IRM) experiments took place at Fort Hoofddijk. A PM-4 pulse magnetizer was used to acquire IRM at 1.0 T. For the first experiment, the samples were bathed in liquid nitrogen ($T = -196$ºC) and immediately put in the PM-4. Directly after imparting IRM, the samples were transferred to the 2G cryogenic magnetometer and measured while warming for at least 15 min. This so-called IRM warm-up experiment (see [22,23]) can indicate variable amounts of superparamagnetic grains. The second experiment is rather similar to the first, but was done at room temperature. We monitored the IRM intensity over a time span of 45 days to detect viscous decay in zero-magnetic field on a laboratory time scale.

2.3.4. Epoxy stirred remanence

We have undertaken redeposition experiments (see e.g., [24,25]) on several samples. After completion of the standard pseudo-Thellier experiment, the sample was stirred in a thin epoxy and hardened for two weeks in the Earth's magnetic field. The (very) short-τ VRM was suppressed through storage in the magnetically shielded room for one day prior to the demagnetization of stirred remanent magnetization (StRM). The results for an NRM–StRM example are shown in Fig. 3. Normalized StRM and ARM as function of AF demagnetizations (upper panel) are very similar in the low fields (0–35 mT), whereas StRM and NRM demagnetizations are more alike in interval 40–95 mT. All remanences are normalized to the highest value. When plotted against each other (middle panel of Fig. 3), NRM and StRM show a rather linear relation between 20 and 60 mT, which we interpret to be the DRM part of the original NRM. The curve tails are ascribed to VRM for low fields, and 'spurious' magnetization acquired during AF demagnetization for high fields. As already expected, the Arai plots (lower panel) for both curves are rather different. Clearly, the StRM curve has a better linearity than the NRM. The NRM decreases more at low fields resulting in a significant VRM

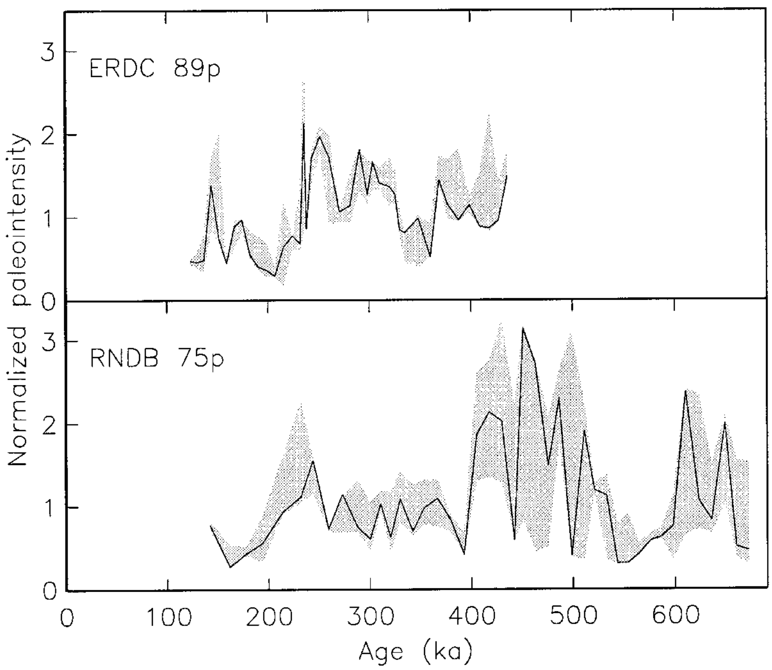

Fig. 2. Results of pseudo-Thellier paleointensity determinations on the cores of this study. Gray areas indicate the central 90% of the jackknife estimates for the best-fit slope.

area. In addition, from the NRM curve in the Arai plot, it is clear that determining the best-fit line for the paleointensity estimate is much less straightforward than for the StRM curve. As a consequence, the y-intercept of the line through the NRM as a possible indicator of VRM (Fig. 1) cannot be determined with high certainty. This experiment suggests that sediments exposed to the Brunhes field for several hundreds of thousands of years can acquire a substantial amount of VRM. Naturally, there is no long-τ VRM when they are redeposited and exposed for a fortnight in the Brunhes field. Stirred remanent magnetization is thus a potential method both to normalize NRM data [24,25] to separate long-τ VRM contributions. It requires accurate and reproducible laboratory experiments, if used as paleointensity determinations for a large set of samples. We found StRM to be highly sensitive to laboratory conditions.

3. VRM area results

From all our pseudo-Thellier measurements on the two cores we have calculated the VRM area. We begin with two examples that indicate the effects of paleoclimate on our VRM area.

3.1. VRM vs. climate

Paleoenvironmental conditions can influence magnetic properties and hence also long-τ VRM acquisition. We illustrate this with two samples from core ERDC 89p, one deposited during an interglacial (stage 11) and one during a glacial (stage 12). Fig. 4a and b indicate rather similar Zijderveld diagrams (because the cores are unoriented, the declinations are not meaningful). Fig. 4c indicates that the normalized remanences have quite different decay curves, whereas the ARM acquisitions are essentially identical, including their absolute values. Normalization has been done using the maximum NRM and ARM values of the sample deposited in the glacial (cold) stage. The Arai plot (Fig. 4d) shows a significant difference between the two samples. The ‘cold’ VRM area is substantially smaller than the ‘warm’ (interglacial) one, which is the sum of the two gray areas. Thus, these examples indicate a strong variation in the demagnetization characteristics of the NRM, and

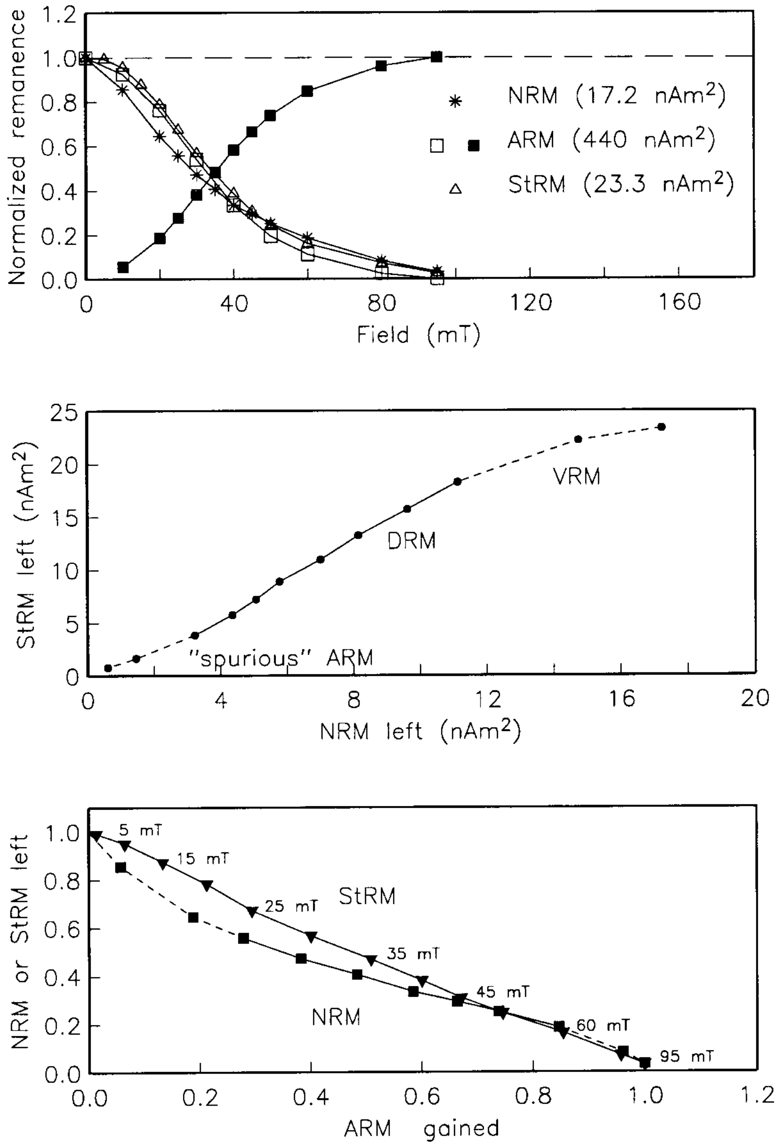

Fig. 3. After the pseudo-Thellier procedure of the NRM, the sediment was redeposited by stirring in epoxy in Earth field (StRM). The middle panel indicates that NRM and StRM are linear between 20 and 60 mT. Low demagnetization fields show a deviating part which we label VRM, and at high AF fields there is evidence for acquisition of spurious magnetization. The StRM versus ARM acquisition (lower panel) is much more linear than the NRM counterpart. In other words, the StRM is suggested to be less affected by long-τ VRM.

this variation is expressed in the VRM areas. Possible reasons for these variations must be sought in climate-related effects. For instance, paleoproductivity has been shown to influence the remanence carrying grains. Hartl et al. [26] suggested that the differences found between the magnetic properties of Eocene and Oligocene sediments of DSDP Site 522 could be ascribed to a variation in reduction diagenesis caused by increased productivity. Their study of a South Atlantic core indicates that rock magnetics can be sensitive indicators of environmental changes. Productivity estimates are also available for a piston core from the Ontong–Java Plateau, taken quite close to ERDC 89p. Herguera [27] showed that the density

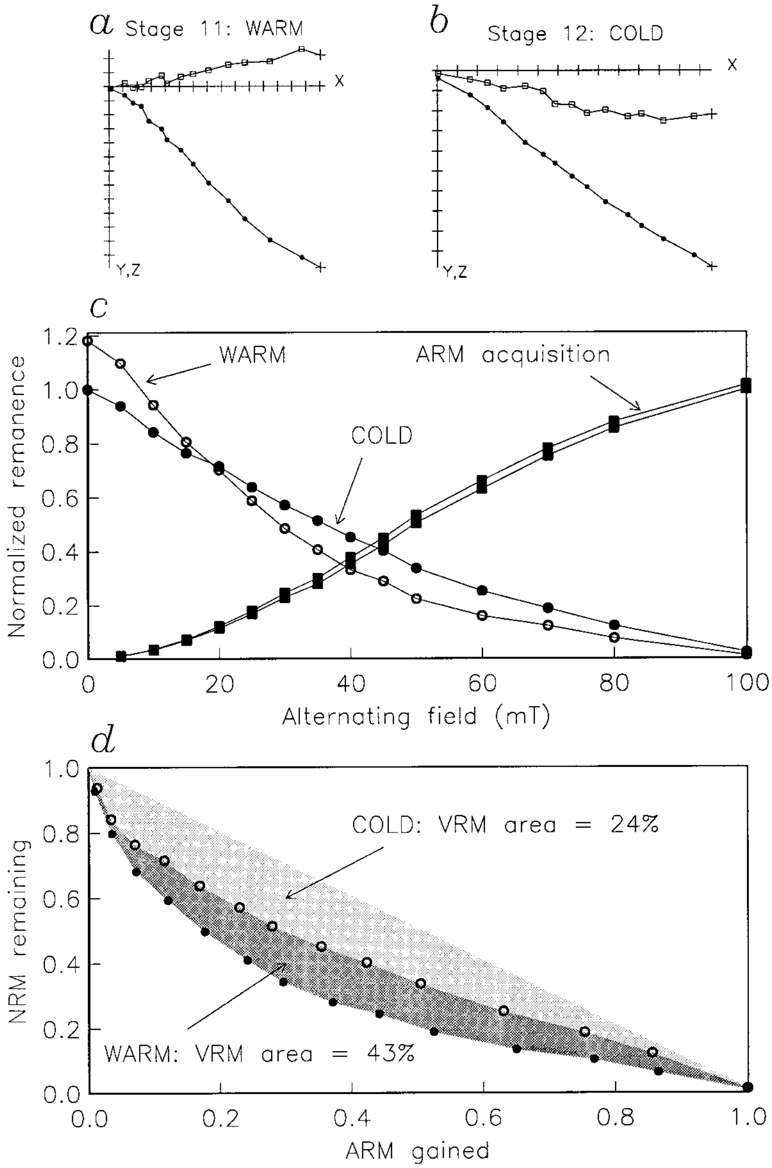

Fig. 4. VRM area determination of a sample deposited during an interglacial (warm) (a) and a glacial (cold) (b) stage. The Zijderveld plots indicate a more or less linear decay towards the origin. (c) NRM demagnetization curves are different, whereas ARM acquisition data are similar. (d) The Arai plot of the NRM versus ARM points out the substantial difference between the two samples; the interglacial period corresponds to a much larger VRM area.

of benthic foraminifera preserved in the sediment correlates well with the climatic $\delta^{18}O$ curve. From his reconstruction it was apparent that glacial periods favor higher productivity (i.e., accumulation of benthic foraminifera), at least for the last 250 kyr. It is possible that these variations in paleoproductivity have influenced the magnetic properties at the ocean floor. It appears that higher productivity intervals are associated with magnetic grain sizes that are more resistant to long-τ VRM, perhaps through dissolution of the finest grains that are most susceptible to VRM. Alternatively, climatically induced factors

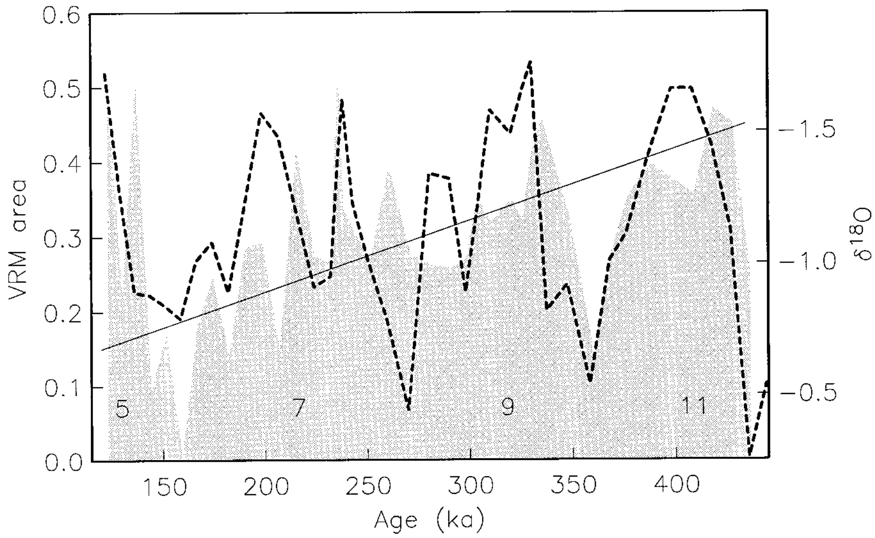

Fig. 5. VRM area (gray) versus age for core ERDC 89p. Links between the $\delta^{18}O$ curve (dashed) and the VRM area are suggested, but an age dependence can be suggested as well. Interglacial stages are indicated by odd numbers.

may cause variations in grain size and provenance of detrital material.

3.2. Core ERDC 89p

Not only the examples shown in Fig. 4, but also data from the entire core ERDC 89p suggest possible links between VRM area and climate as represented by $\delta^{18}O$ (Fig. 5). Possibly, a superimposed $\delta^{18}O$ pattern on an apparent age-dependent trend is observed in the VRM area. The long-term trend is consistent with viscous relaxation of magnetization [2,9], but also with the mechanical model of Mazaud [28] that suggests progressive acquisition of post-detrital magnetization in the first meters of the core.

3.3. Core RNDB 75p

The other Ontong-Java Plateau core (RNDB 75p) also shows a trend in the VRM area versus age between 400 and 140 ka (Fig. 6). As already noted by Tauxe and Shackleton [19], its magnetic properties change abruptly approximately half way down the core (at about 4 m, or 400 ka). The oldest part, which is less ideal for paleointensity research, shows more viscous behavior (significantly larger inferred VRM) than the younger part. Furthermore, some high-frequency components in the oxygen isotope signature correspond well to variations in the VRM area.

The difference between the upper and lower half of this core is evident from the saturation IRM versus susceptibility χ plot of Tauxe and Shackleton [19] (see Fig. 7). The data fall on two distinct tracks which they ascribed to a change in grain size. To illustrate this, a best-fit line through the 'upper track' was calculated [19]. From this they estimated an IRM value from a given χ value. The differences between these 'expected' IRM values and the observed IRM values were called ΔIRM, and are a measure of the influence of grain size. In Fig. 8 the ΔIRM values are plotted together with the VRM area data. The correlation between ΔIRM and VRM area is remarkably good. The trend in the youngest part of the VRM area record seems to correspond to a slight trend in the ΔIRM, which could suggest that this VRM area trend is controlled in part by diagenetic phenomena, as opposed to strictly age-related growth.

The two tracks in the IRM versus χ data [19] are controlled by enhanced χ in the lower part of the core. This could be the result of either larger grains (multi-domain range), or additional superparamagnetic (SP) particles. SP behavior at room (or ocean) temperature can be detected by IRM warm-up experiments (see [22,23,26]. SP grains carry remanence

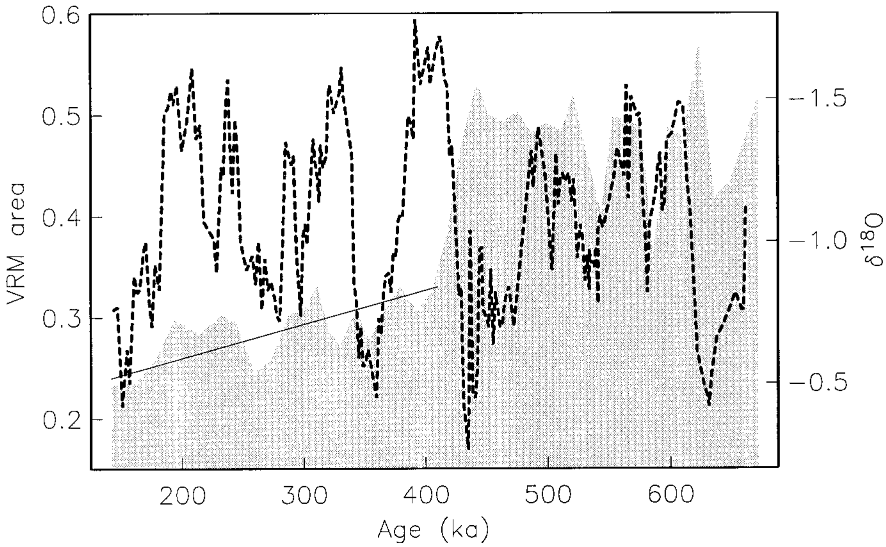

Fig. 6. VRM area (gray) versus age for core RNDB 75p. The youngest half shows an age-dependent trend in VRM area data. The oldest part of this record has a slightly different grain size [19], which is also evident from the significant difference in VRM area. Correspondence between $\delta^{18}O$ and VRM area are mainly observed in the oldest 150 kyr.

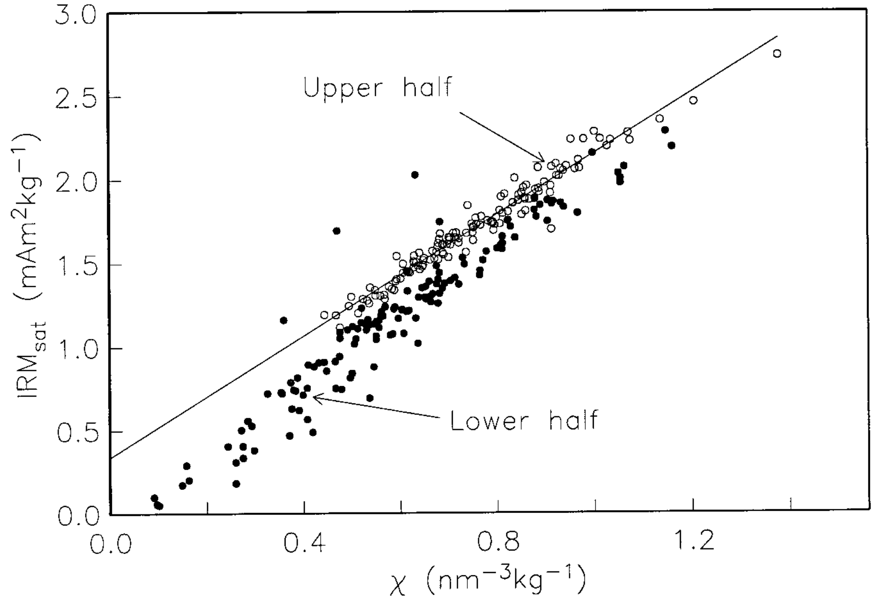

Fig. 7. Saturation IRM against low-field magnetic susceptibility. The data fall on two well-defined tracks for samples of either half of the core. (Redrawn from [19].)

at liquid nitrogen temperature and lose it during the warm-up to room temperature. An IRM imparted at $T = -196$ºC will show a greater loss of intensity if more SP grains are present. Because the first measurements did not all occur at exactly the same time since the magnetization was acquired, we choose to normalize the IRM intensity with the measured value after 180 s (this does not effect the outcome of the experiment). The results of the IRM warm up experiments are shown in Fig. 9. It is clear that

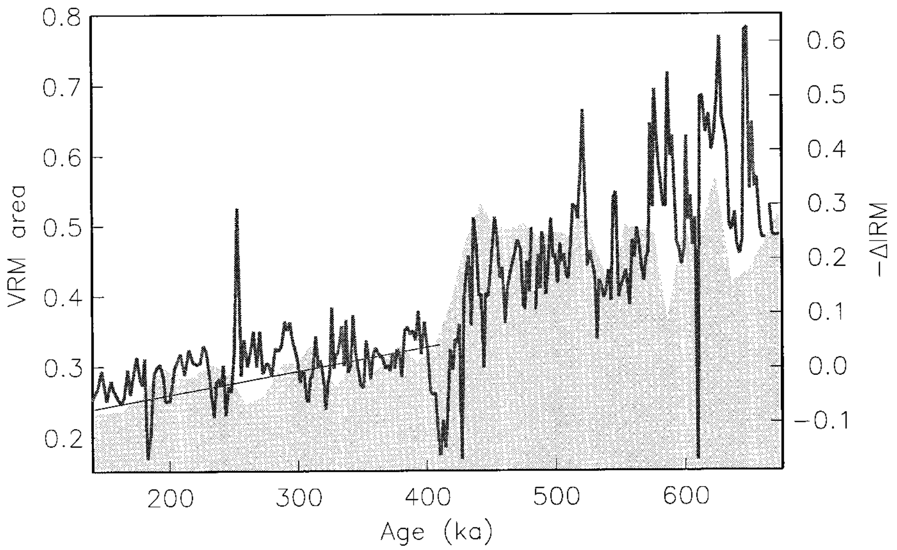

Fig. 8. The difference ΔIRM between the measured saturation IRM and the value predicted from a given χ [19] indicates the same behavior as the VRM area for core RNDB 75p.

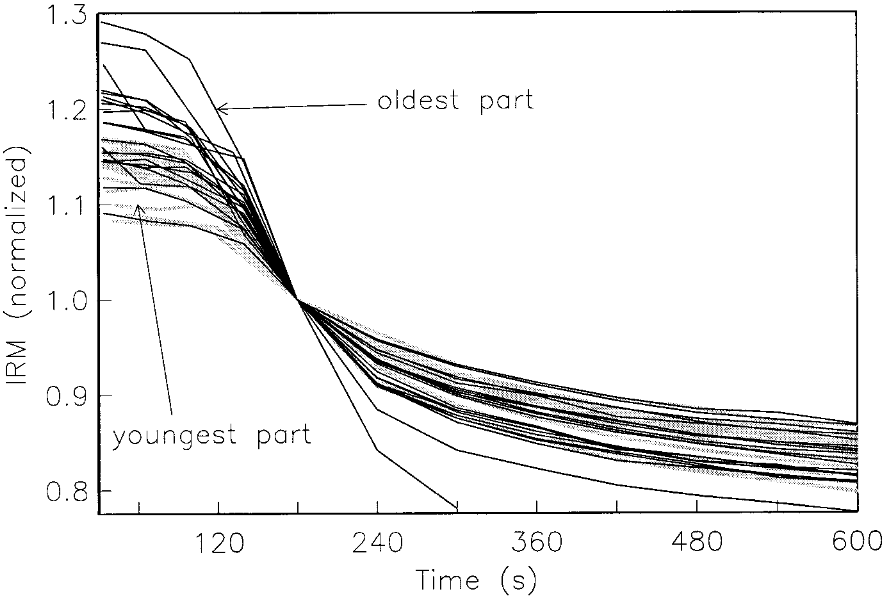

Fig. 9. Curves of IRM imparted at liquid nitrogen temperature versus time for core RNDB 75p. The data are normalized to IRM readings after 180 s. The oldest part (black) of the record indicates a greater loss of moment than the youngest part (gray), consistent with a greater portion of super-paramagnetic grains.

samples from the oldest part of core RNDB 75p exhibit a greater loss of IRM intensity on warming up, implying that the oldest part of the core has a higher concentration SP grains. We suggest that the enhanced SP concentration in the lower half of the core is accompanied by an enhancement of longer relaxation time grains, leading to an overall higher long-τ VRM contribution.

4. Short-τ VRM

A link between long- and short-τ VRM was implied in the pseudo-Thellier approach [16]. In that study, the long-τ VRM contribution was defined as the difference between the conventional paleointensity estimate (estimated by a blanket demagnetization and normalization) and the slope in the Arai plot. The decay of a saturation IRM intensity in zero field after 3.5 h was taken as the short-τ viscous behavior. Both viscous parameters correlated well, which supported the assumption that the pseudo-Thellier detects and removes VRM. The drawbacks of this approach are that the conventional paleointensity determination depends on a single NRM reading and that the 'real' relative paleointensity must be reliably determined. We now test our improved long-τ VRM estimates — that do not suffer from these problems — against the shorter-term viscous effects. All samples from core RNDB 75p were therefore subjected to an IRM decay experiment.

The first measurements (some 20 s after IRM acquisition) are used to normalize the subsequent measurements after 1, 6, 9, and 45 days. Fig. 10 shows the behavior of IRM remaining as a function of time for all samples. IRM remaining varies from 99.5% to 91.5% of the initial IRM intensities. The elapsed time is on a logarithmic scale, therefore, the IRM decay is more or less $\log(t)$.

In Fig. 11 we plot the same IRM-remaining data as function of age, and compare these to the VRM area. After one day, we observe small variations in the percentages of IRM left, that could be correlated to variations in the VRM area. After 6 and 9 days, the correspondence became slightly better, but we also noted that the oldest part had decayed more than the youngest. The last measurements occurred after 45 days; the separation between upper and lower half is more clear. It supports the contention that short-τ viscous effects of the IRM decay (in the order of weeks) are related to what we think is the long-τ VRM acquisition (in the order of hundreds of thousands of years). We note that in cases where long- and short-term VRM estimates are not similar a very soft viscous overprint may be the culprit (as discussed in Section 2.2). Furthermore, diagenetic effects like possible biological iron growth could have biased either ARM or IRM decay data. In conclusion, the oldest part of RNDB 75p has more VRM, both short-τ and long-τ.

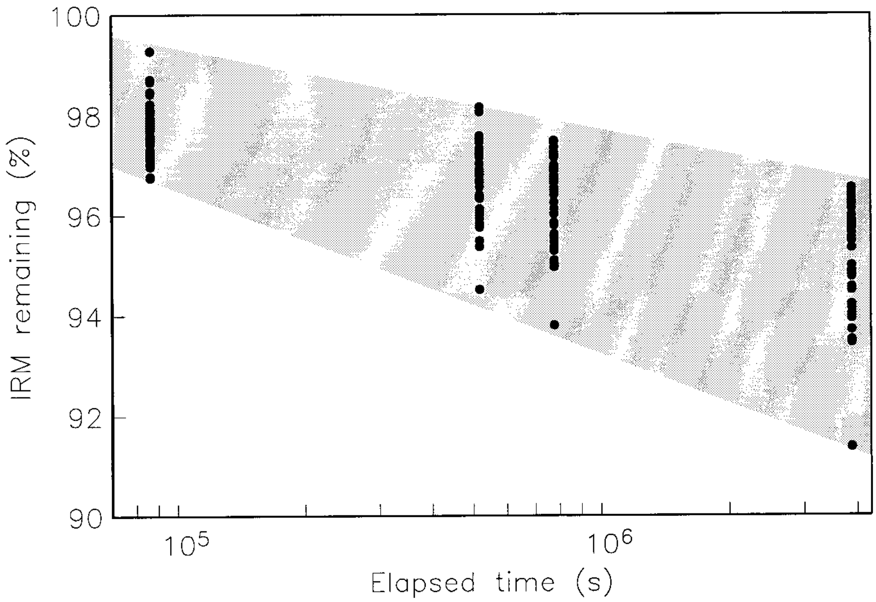

Fig. 10. IRM decay in zero field as a function of elapsed time (on logarithmic scale) for samples of RNDB 75p. The values are normalized by the first measurements (100%).

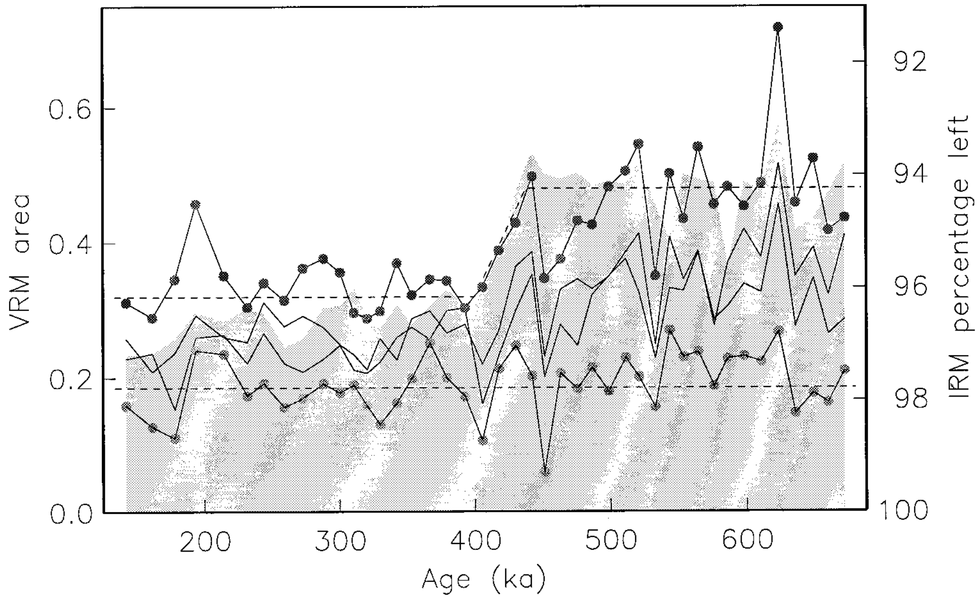

Fig. 11. Viscous decay of IRM as function of age, together with the VRM area values for core RNDB 75p. Gray symbols: after 1 day; black symbols: after 45 days; black lines: after 6 and 9 days. Dashed lines suggest that IRM decay after 45 days is linked with long-τ VRM. Note that the IRM percentages are plotted upside-down.

5. Conclusions

Acquisition of VRM occurs in all rocks and is, mostly, an unwanted relaxation process of the total NRM. Short-τ VRM contributions are often suppressed by storage in a magnetically shielded space or by rather weak demagnetization levels. On the other hand, viscous remanences acquired over a long time span (several 100 thousand years) are harder to separate from primary magnetizations, also because they are often parallel (or anti-parallel) to DRM. Especially in paleointensity studies, one must be certain to have eliminated VRM as well as other secondary magnetizations before paleointensity can be extracted.

We have developed a method to characterize long-τ viscous processes of sedimentary natural magnetic remanences. It uses the pseudo-Thellier paleointensity technique described [16] that connects NRM demagnetization with ARM acquisition. When NRM is plotted against ARM, we typically observe a concave-up curve, whose curvature is quantified by the ‘VRM area’ (Fig. 1). We propose that this VRM area is an indication of long-τ VRM that has built up since deposition.

The VRM area data of the two cores studied here indicate three characteristics: (1) a long-τ decaying trend which is explained as the growth of VRM with time, (2) a link with climate ($\delta^{18}O$ data) where warm periods often correspond to relatively high VRM estimates, and (3) a stronger link with a lithological change, presumably diagenetic in origin, that is confirmed with viscous effects on laboratory time scales.

Acknowledgements

We thank Cor Langereis, Alain Mazaud and Martha Schwartz for comments and suggestions that improved the manuscript. The investigations were supported by the Netherlands Geosciences Foundation (GOA) with financial aid from the Netherlands Organization for Scientific Research (NWO) (750.194.09). Further financial support was provided by National Science Foundation (NSF) (EAR9706019). ***[RV]***

References

[1] L. Tauxe, Sedimentary records of relative paleointensity of the geomagnetic field in sediments: theory and practice, Rev. Geophys. 31 (1993) 319–354.

[2] L. Néel, Théorie du trainage magnétique des ferromagnétiques en grains fins avec applications aux terres cuites, Ann. Geophys. 5 (1949) 99–136.

[3] L. Néel, Some theoretical aspects of rock magnetism, Adv. Phys. 4 (1955) 191–243.

[4] D.J. Dunlop, Theory of magnetic viscosity of lunar and terrestrial rocks, Rev. Geophys. Space Phys. 11 (1973) 855–901.

[5] D.J. Dunlop, Viscous magnetization of 0.04–100 μm magnetites, Geophys. J.R. Astron. Soc. 74 (1983) 667–687.

[6] D.J. Dunlop, Ö. Özdemir, Rock Magnetism: Fundamentals and Frontiers, Cambridge University Press, 1997.

[7] W. Lowrie, Viscous remanent magnetization in oceanic basalts, Nature, 243 (1973) 27–29.

[8] G. Pullaiah, E. Irving, K.L. Buchan, D.J. Dunlop, Magnetization changes caused by burial and uplift, Earth Planet. Sci. Lett. 28 (1975) 133–143.

[9] Y.S. Kok, L. Tauxe, Saw-toothed pattern of relative paleointensity records and cumulative viscous remanence, Earth Planet. Sci. Lett. 137 (1996) 95–99.

[10] J.-P. Valet, L. Meynadier, Geomagnetic field intensity and reversals during the past four million years, Nature, 366 (1993) 234–238.

[11] Y.S. Kok, L. Tauxe, Saw-toothed pattern of sedimentary paleointensity records explained by cumulative viscous remanence, Earth Planet. Sci. Lett. 144 (1996) E9–E14.

[12] J.W. King, S.K. Banerjee, J. Marvin, A new rock magnetic approach to selecting sediments for geomagnetic paleointensity studies: application to paleointensity for the last 4000 years, J. Geophys. Res. 88 (1983) 5911–5921.

[13] E. Thellier, O. Thellier, Sur l'intensité du champ magnétique terrestre dans le passé historique et géologique, Ann. Geophys. 15 (1959) 285–378.

[14] R.S. Coe, The determination of paleo-intensities of the Earth's magnetic field with emphasis on mechanisms which could cause non-ideal behavior in Thellier's method, J. Geomag. Geoelectr. 19 (1967) 157–178.

[15] P. Hartl, L. Tauxe, A precursor to the Matuyama/Brunhes transition-field instability as recorded in pelagic sediments, Earth Planet. Sci. Lett. 138 (1996) 121–135.

[16] L. Tauxe, T. Pick, Y.S. Kok, Relative paleointensity in sediments; a pseudo-Thellier approach, Geophys. Res. Lett. 22 (1995) 2885–2888.

[17] T. Nagata, Y. Arai, K. Momose, Secular variation of the geomagnetic total force during the last 5000 years, J. Geophys. Res. 68 (1963) 5277–5282.

[18] L. Tauxe, G. Wu, Normalized remanence in sediments of the Western Equatorial Pacific: relative paleointensity of the geomagnetic field?, J. Geophys. Res. 95 (1990) 12337–12350.

[19] L. Tauxe, N.J. Shackleton, Relative paleointensity records from the Ontong-Java Plateau, Geophys. J. Int. 117 (1994) 769–782.

[20] J. Imbrie, J.D. Hays, D.G. Martinson, A. McIntyre, A.C. Mix, J.J. Morley, N.G. Pisias, W.L. Prell, N.J. Shackleton, The orbital theory of Pleistocene climate: support from a revised chronology of the marine $\delta^{18}O$ record, in: A.L. Berger, J. Imbrie, J. Hays, G. Kukla, B. Saltzman (Eds.), Milankovitch and Climate, 1, Reidel, Dordrecht, 1984, pp. 269–305.

[21] N.J. Shackleton, A. Berger, W.R. Peltier, An alternative astronomical calibration of the lower Pleistocene time scale based on ODP Site 677, Trans. R. Soc. Edinburgh Earth Sci. 81 (1990) 251–261.

[22] S.L. Halgedahl, R.D. Jarrard, Paleomagnetism of the Kuparuk River formation from oriented drill core: evidence for rotation of the Alaska Plate, in: I. Tailleur, P. Wymer (Eds.), Alaskan North Slope Geology, Society of Economic Paleontologists and Mineralogists, Pacific Section, Bakersfield, CA, 1987, pp. 581–617

[23] T. Pick, L. Tauxe, Holocene paleointensities: Thellier experiments on submarine basaltic glass from the East Pacific Rise, J. Geophys. Res. 98 (1993) 17949–17964.

[24] P. Tucker, Stirred remanent magnetization: a laboratory analogue of post-depositional realignment, J. Geophys. 48 (1980) 153–157.

[25] P. Tucker, Paleointensities from sediments: normalization by laboratory redepositions, Earth Planet. Sci. Lett. 56 (1981) 398–404.

[26] P. Hartl, L. Tauxe, T. Herbert, Earliest Oligocene increase in South Atlantic productivity as interpreted from 'rock magnetics' at Deep Sea Drilling Project Site 522, Paleocanography, 10 (1995) 311–325.

[27] J.C. Herguera, Nutrient, mixing and export indices: a 250 kyr paleoproductivity record from the western equatorial Pacific, in: R. Zahn (Ed.), Carbon Cycling in the Glacial Ocean: Constraints on the Ocean's Role in Global Change, NATO ASI Series, I, 17, Springer-Verlag, 1994, Berlin, pp. 481–519.

[28] A. Mazaud, 'Sawtooth' variation in magnetic intensity profiles and delayed acquisition of magnetization in deep sea cores, Earth Planet. Sci. Lett. 139 (1996) 379–386.